HHS Public Access

Author manuscript

*Nat Med*. Author manuscript; available in PMC 2018 May 01.

Published in final edited form as:

*Nat Med*. 2017 November ; 23(11): 1271–1276. doi:10.1038/nm.4411.

# Defining Total Body AIDS Virus Burden: Implications for Curative Strategies

**Jacob D. Estes, PhD**[1], **Cissy Kityo, MD**[2], **Francis Ssali, MD**[2], **Louise Swainson, PhD**[3], **Krystelle Nganou Makamdop, PhD**[4], **Gregory Q. Del Prete, PhD**[1], **Steven G. Deeks, MD**[5], **Paul Luciw, PhD**[6], **Jeffrey Chipman, MD**[7], **Gregory Beilman, MD**[7], **Torfi Hoskuldsson, MD**[7], **Alexander Khoruts, MD**[8], **Jodi Anderson**[8], **Claire Deleage**[1], **Jacob Jasurda**[8], **Thomas Schmidt**[8], **Michael Hafertepe**[8], **Samuel Callisto**[8], **Hope Pearson**[8], **Thomas Reimann**[8], **Jared Schuster**[8], **Jordan Schoephoerster**[8], **Peter Southern, PhD**[9], **Katherine Perkey**[9], **Liang Shang, PhD**[9], **Steve Wietgrefe**[9], **Courtney V. Fletcher, Pharm D**[10], **Jeffrey D. Lifson, MD**[1], **Daniel C. Douek, MD PhD**[4], **Joseph M. McCune, MD PhD**[3], **Ashley T. Haase, MD**[9], and **Timothy W. Schacker, MD**[8,*]

[1]AIDS and Cancer Virus Program, Frederick National Laboratory for Cancer Research, Leidos Biomedical Research, Inc., Frederick, MD [2]Joint Clinical Research Center, Kampala, Uganda [3]Division of Experimental Medicine, University of California, San Francisco, CA [4]Vaccine Research Center, National Institutes of Health, Bethesda, MD [5]Department of Medicine, University of California, San Francisco, San Francisco, CA [6]Department of Pathology and Laboratory Medicine, University of California, Sacramento, CA [7]Department of Surgery, University of Minnesota, Minneapolis, MN [8]Department of Medicine, University of Minnesota, Minneapolis, MN [9]Department of Microbiology and Immunology, University of Minnesota, Minneapolis, MN [10]College of Pharmacy, University of Nebraska Medical Center, Omaha, NE

## Abstract

In the quest for a functional cure or eradication of HIV infection, we need to know how large the reservoirs are from which infection rebounds when treatment is interrupted. To that end, we quantified SIV and HIV tissue burdens in tissues of infected non-human primates and lymphoid tissue (LT) biopsies from infected humans. Before antiretroviral therapy (ART), LTs harbor more than 98 percent of the SIV RNA+ and DNA+ cells. While ART substantially reduced their numbers, vRNA+ cells were still detectable and their persistence was associated with relatively low drug concentrations in LT compared to peripheral blood. Prolonged ART also reduced the

[*]Corresponding Author: Timothy Schacker, MD, Department of Medicine, MMC250, 420 Delaware Street SE, Minneapolis, MN 55455, Phone: 612-624-9955, Schacker@UMN.edu.

**Author Contributions:** JDE contributed to study design and oversight, sample analysis, and manuscript preparation. CK contributed to study design, oversight of Uganda Cohort, and manuscript preparation. FS contributed management of Ugandan cohort including regulatory and sample management. LS, GQDP, JA, CD, JJ, TS, MH, SC, HP, TR, JS, JS, KP contributed to sample analysis. PS contributed to sample and data analysis. KNM contributed to sample collection and analysis and data management. JC, GB, and TH performed surgery to collect LN and rectal samples from the Ugandan cohort. AK contributed with sample collection and study design. LS performed the TSA/ELF assays and analysis. SW contributed data analysis and technical support. CVF contributed drug level data, sample analysis, and manuscript preparation. SGD, PL, JDL, DCD, JMM, ATH, and TWS contributed to study design, data analysis, and manuscript preparation

**Competing Interests**

There is NO Competing Interest.

level of SIV and HIV-DNA+ cells, but the estimated size of the residual tissue burden of $10^8$ vDNA+ cells that potentially harbor replication competent proviruses, along with the evidence for continuing virus production in LT despite ART, identify two important sources for rebound following treatment interruption. The large sizes of these tissue reservoirs underscore the challenges in developing “HIV cure” strategies that target multiple sources of virus production.

## Introduction

The quest for cure of HIV infection was inspired by Timothy Ray Brown, an HIV-infected individual who in the course of treatment for refractory leukemia with total body irradiation and chemotherapy, also received two bone marrow transplants with CCR5 delta 32 mutated HIV-resistant cells, a combination of reduced HIV reservoirs and resistant cells thought to have not only cured his leukemia but HIV infection as well[1]. The success in Mr. Brown’s case, albeit achieved with a highly toxic treatment, has galvanized the field to seek a functional cure (i.e., a prolonged period off ART without detectable plasma viremia) or HIV eradication, by safer and more scalable approaches.

What are the cellular and anatomic compartments from which infection might rebound off ART to achieve a functional cure or eradication? To answer this question, we undertook an extensive analysis of potential sources of viral rebound, using both established and next generation *in situ* hybridization (ISH) technologies and quantitative image analysis (QIA). We paid particular attention to lymphoid tissues (LT) in HIV and SIV infections, in which it has been previously shown that CD4+ T cells in the gut and secondary LT are the principal sites where most of the viral (v)RNA+ virus-producing cells are found in HIV infected humans and SIV infected macaques[2-18]; and where there is a very large pool (more than $10^{10}$ cells) of transcriptionally-silent vDNA+ cells in LT[3], some of which contain replication-competent proviruses.

While previous characterization of HIV and SIV infected tissues had clearly identified LT and the vDNA+ and vRNA+ cells therein as important anatomic sites and cellular sources of virus potentially capable of reigniting infection following treatment interruption[2-4,7,14,16,18,19], much of this work was done during the 1990’s prior to modern antiretroviral therapy (ART). Our understanding of the extent to which current ART regimens impact virus burden in LT and other tissues is therefore incomplete. Moreover, there is recent evidence that even contemporary ART regimens that suppress viral replication sufficiently to reduce plasma viremia to levels below the sensitivity of clinical laboratory assays, achieve drug levels in LT that are comparatively lower than the fully suppressive drug levels in peripheral blood (PB)[5]. These lower tissue drug levels were correlated with incomplete suppression of viral replication in LT in some patients[19,20]. There is also growing appreciation that the size of the pool of latently infected cells that may contribute to viral rebound after treatment interruption has been underestimated by as much as 70-fold[21]. There are thus three good reasons to re-examine potential sources of rebound when ART is interrupted.

To identify the sources of potential viral rebound, we conducted extensive analysis of necropsy tissues from rhesus macaques (RM) infected with SIVmac251, SIVmac239, or RT-

SHIV, using new facile techniques of DNAscope and RNAscope ISH to quantify vDNA+ and vRNA+ cells[22]; a previously published ISH method employing tyramide signal amplification (TSA) to score for virus producing cells[23]; and measures of the intracellular concentration of ART drugs and/or active metabolites to assess associations between suboptimal tissue drug concentrations and ongoing replication during ART. In HIV infection, we examined LT reservoirs in serial lymph node (LN) and gut biopsies obtained prior to and after at least 2 years of ART in HIV-infected people. We show in the non-human primate (NHP) model, that in the absence of ART, >98% of detectable vRNA+ and vDNA+ cells were found in LT. ART reduced the frequency of vRNA+ cells, but, despite apparently clinically effective ART (plasma vRNA < 50 copies/mL), we also found vRNA+ cells in every organ system examined. In LN where tissue levels of ART drugs are substantially lower than in PB, we show that virus-producing cells remain detectable; and we provide new estimates of how large the pool of vDNA+ cells in LT with replication competent proviruses might be. The persistence of virus-producing cells on ART and a large pool of vDNA+ cells with the potential to become reactivated underscores the challenges of HIV eradication.

## Results

### NHP studies

We analyzed brain, gut, heart, kidney, liver, lungs, LN, and spleen tissues collected at necropsy from eight RM infected with SIVmac251 (3 untreated, 5 on ART) housed at Advanced Bioscience Laboratories (ABL). The three untreated SIVmac251-infected animals were euthanized and necropsied 14, 43 or 90 days post-infection (dpi). The remaining five SIVmac251 infected animals were euthanized and necropsied after 20-22 weeks of treatment with raltegravir, darunavir, ritonavir, emtricitabine, and tenofovir started at 56 dpi (Supplementary Figure 1A). We also analyzed LN from 11 SIVmac239 infected RM housed at the National Institutes of Health (NIH) on suppressive ART regimens (described in the methods section and previous publications[22,24,25], Supplementary Figure 1B, C); and tissues from four untreated RT-SHIV infected juvenile RM housed at the California National Primate Research Center (CNPRC) euthanized and necropsied at 19, 24, 41 or 69 weeks after infection and tissues from 4 RT-SHIV-infected juvenile RM from CNPRC after a minimum of 26 weeks of ART with a combination of efavirenz, emtricitabine, and tenofovir[26] (Supplementary Figure 1D). Collectively, we assessed the tissue viral burden in 27 RMs infected with three distinct simian AIDS viruses.

### Reservoir measurements by ISH

We used ISH technologies and quantitative image analysis (QIA) to define tissue reservoirs in SIV/SHIV and HIV infections as numbers of vDNA+, vRNA+ and virus producing cells. These cellular measurements thus define reservoirs in a different way than PCR and RT-PCR analysis of nucleic acids extracted from homogenized whole tissues, where there will be ambiguity in attributing the number of copies of vDNA or vRNA to a large number of cells with a few viral copies, or to a small number of cells with a large number of viral copies. We used four methods of ISH: 1) $^{35}$S radio-labeled riboprobes that hybridize to regions that span the genome of SIV/SHIV (*gag*, *pol*, *vif*, and *vpr*, *env* and *nef*) to detect transcriptionally active vRNA+ cells that we have previously shown to contain both unspliced and spliced

vRNAs[8]; 2) digoxygenin-labelled riboprobes combined with TSA amplification to reveal virus producing cells at the light microscopic level[23]; 3) RNAscope ISH, a more rapid ISH technique as sensitive and specific as the $^{35}S$ technique[22] to determine the frequency of vRNA+ cells/g tissue; and 4) DNAscope ISH[22] to measure the frequency and location of vDNA+ cells. DNAscope enables sensitive detection and quantitation of vDNA+ cells comparable to *in situ* PCR[2,3], but with greater speed, convenience and increased spatial resolution of vDNA signal within the infected cell. We compared the frequency of vRNA+ and vDNA+ cell/g LT to measures of vRNA and vDNA by qRT-PCR and qPCR, and found excellent agreement ($R^2$ =0.89 and $p < 0.0001$ for RNA and $R^2$ =0.73 and $p < 0.0001$ for DNA, Supplementary Figure 2). The agreement with similar recently published results[22] provides further justification of this approach to quantitate viral reservoirs on a cellular basis.

## SIV RNA+ cells are mainly in lymphoid tissues

We quantitatively characterized cellular tissue reservoirs in untreated SIV infection in the brain, heart, kidney, liver, lungs, spleen, LN (axillary, colonic, inguinal, and mesenteric), and multiple sites in the gut (duodenum, jejunum, ileum, ascending and transverse colon, and rectum), and show in Supplementary Figure 3 representative images of SIV *in situ* hybridization from multiple tissues using two complimentary approaches. We analyzed serial 4μm sections of formalin fixed, paraffin embedded tissues, evaluating every fifth section in at least five sections total to provide analysis through ≥ 80μm of each tissue. The frequency of SIV RNA+ cells was determined in each section and converted to the frequency per gram (g) from the measured area of the section, nominal thickness, and previously determined density of fixed tissue of ~ 1g/cm$^3$ [16]. For example, the frequency of vRNA+ cells/μm$^2$ area × 4μm thick=vRNA+ cells/μm$^3$ × $10^{12}$ μm$^3$/cm$^3$ × 1gm/cm$^3$ = vRNA + cells per gram of tissue.

The density of vRNA+ cells was highest in LT, but vRNA+ cells were detected in every organ, including the heart, liver, kidney, and central nervous system. To estimate total viral burden for different tissues, we assumed that each organ contributes vRNA+ cells to the total population of vRNA+ cells proportional to the frequency of vRNA+ cells measured by ISH and the total mass of these organs. In the rhesus macaque studied at peak viremia, for example, the mass of the heart was approximately 38.3 grams and the frequency of vRNA+ cells was 7.54 × $10^3$ cells/gram, thus the total number of infected cells in this organ was accordingly estimated at ~2.89 × $10^5$ cells (Supplementary Table 1). The combined mass of lymph nodes for this animal was estimated to be 78 grams (~1% of total body mass). With a mean frequency of ~8.73 × $10^5$ vRNA+ cells/gram, the total population of vRNA+ cells in LNs was estimated at 7.68 × $10^7$ cells, approximately 2 $\log_{10}$ higher than found in the heart. In the gut, we measured ~5.57 ×$10^5$ vRNA+ cells/g so that from the total organ weight of 315 grams in this animal, ~1.68 c$10^8$ vRNA+ cells or more than two-thirds of the total number of vRNA+ cells in all of the organs examined were in the gut. In Figure 1, we show graphically the contribution of each organ to the estimated total population of infected cells (as a percentage of the total) before and during ART, to illustrate the fact that the primary reservoir sites of infection are LTs, where ~98.4% of vRNA+ cells reside (gut, LNs, and spleen). The addition of the lungs, a tissue with abundant mucosal associated lymphoid

tissue (MALT), increases our estimate of the frequency of vRNA+ cells residing in LTs to ~99.6%.

### vRNA+ and vDNA+ cell populations are established in LT reservoirs in early infection

We investigated differences in the frequency of viral nucleic acid positive cells by anatomic site and duration of untreated SIVmac251 infection in 4 LNs (axillary, colonic, inguinal, and mesenteric) and from multiple sites in the gut (duodenum, jejunum, ileum, ascending colon, transverse colon, and rectum) in the acute (14 dpi), early (43dpi) and later chronic stages (90 dpi) of infection. In LN and gut, vRNA+ cells were detected in early infection, and only varied by approximately 0.5 log (Figure 2A, B) showing remarkable consistency between LN located in different anatomic locations. The estimated frequency of vDNA+ cells in LT in the SIVmac251-infected animals, assessed using SIV DNAscope (Figure 2 C, D and Supplementary Figure 4), also shows that substantial pools of vDNA+ cells are established early and maintained at high levels in the chronic stages of infection in rhesus macaques.

### Impact of ART on vRNA and vDNA+ cell populations in tissues

In SIVmac251-infected RM that received 20-22 weeks of ART beginning at 56 dpi the frequency of vRNA+ cells were reduced by approximately 2 $\log_{10}$ in LN compared to untreated infection (Figure 3A and supplementary Table 2 A-D), but only about two-fold or less in gut and spleen. The frequency of vRNA+ cells was actually higher in the brains of animals receiving ART compared to untreated animals, presumably reflecting inter-animal variability (supplementary Table 2A), and poor penetration of drugs into the brain. In the RT-SHIV-infected animals, 26 weeks of ART reduced the number of vRNA+ cells by ~3 to 4 $\log_{10}$ in all LT, but only about two-fold in the brain (Figure 3B). The greater reductions seen in the RT-SHIV infected animals compared to SIV infected animals may reflect the relative effectiveness of the different ART regimens against the respective target viruses, distinct differences in viral replication capacity in RM, differences in tissue concentrations of ART, or Env-specific immune responses.

We have previously shown in HIV-infected humans that the intracellular concentration of antiretroviral drugs (ARVs) in LT can be significantly less than concentrations in PBMC, and well below the optimal concentration for virus suppression[5]. We measured intracellular concentrations of ARVs in PBMC, and cells of the LN, ileum (gut associated lymphoid tissue, GALT) and rectal-associated mucosal tissue (RALT) from 6 of the animals described above and similarly found lower ART concentration in LT compared to blood (Figure 4). The median ratio for tenofovir-diphosphate (TFV-DP, an active phosphorylated form of drug) in LN:PBMC was 0.84; 0.41 for GALT:PBMC; and 0.84 for RALT:PBMC. The median ratios for emtricitabine-triphosphate (FTC-TP) were 0.26 LN:PBMC; 0.32 GALT:PBMC; and 0.32 for RALT:PBMC. The median RALT:PBMC ratio for darunavir (DRV) was 15; however DRV was not quantifiable in LN or GALT samples. Thus, in none of the compartments studied were concentrations of the ARVs equivalent to those in peripheral blood, with the exception of DRV in RALT (see Supplementary Table 3 for a summary of intracellular concentration of ARVs for all drugs studied). These results support the hypothesis that comparatively lower antiretroviral (ARV) concentrations in different tissues could contribute to incomplete suppression of viral replication in those tissues.

With the exception of the heart, vRNA+ cells were detectable in every animal on ART, even though all had plasma viral loads (pVL) < 50 copies/mL (the limit of detection for the assay used). The highest numbers of vRNA+ cells during ART were mainly in LTs (lymph node, spleen and GALT) and the lung. Since detection of vRNA+ cells signifies transcription and not necessarily virus production, we used ISH/TSA amplification using an enzyme linked immunofluorescence technique (ELF97) to detect virus producing cells at the light microscopic level[23] to show that vRNA+ cells were also producing virus during ART. We measured the frequency of vRNA+ cells by RNAscope and the frequency of cells producing virions by TSA/ELF97 in 20 subjacent sections from two of the SIVmac 251 infected animals on suppressive ART for > 6 months (Figure 5). There was good agreement between the two measures (Supplementary Table 4) consistent with the conclusion that most vRNA+ cells detected in LN are producing virions.

We used DNAscope to assess the impact of ART on the frequency of vDNA+ cells in 11 SIVmac239-infected animals that had been treated for a mean of 30 weeks (range 25-35 weeks) beginning at 4 wpi (Figure 3C and Supplementary Figure 4). Prior to ART the mean frequency of vDNA+ cells were ~$1 \times 10^7$ cells/g LT. ART reduced the mean frequencies of vDNA+ cells/gram by ~1.7 $\log_{10}$ to ~$3.5 \times 10^5$ cells/g LT. Thus, there is a very large residual reservoir of vDNA+ cells during ART, the implications of which we later discuss.

## HIV RNA+ and DNA+ cells in LT

To compare residual virus levels in LT in SIV infection with HIV infection of humans, we analyzed LN and rectal samples collected before ART and after at least two years of ART from a cohort of 20 individuals in Kampala, Uganda. These individuals had advanced infection when ART was begun, consistent with treatment guidelines in Uganda at the time tissues were obtained. The average age of this cohort at entry was 32 years and 50% were women. The mean CD4+ T cell count at study entry was 174 cells/$mm^3$ (range 30-309 cells/$mm^3$) and the mean plasma HIV viral load was $8.1 \times 10^4$ copies/ml (range $7.4 \times 10^2$ – $9.1 \times 10^5$ copies/ml). The individual changes in CD4 and pVL over time for a subset of 14 individuals followed longitudinally can be found in Supplementary Figures 5 and 6 (respectively).

Based on preliminary analyses in which we found that Clade B riboprobes detected fewer vRNA+ cells than riboprobes for the prevalent Clades A and D in Uganda (not shown), we designed Clade A and D specific RNAscope and DNAscope probes for this study. With these probes we determined an average frequency of vRNA+ cells in LN and rectum prior to ART of ~$9.4 \times 10^4$ cells/gram ($6.3 \times 10^3$ – $3.5 \times 10^5$ cells/gram) and ~$2.5 \times 10^5$ cells/gram ($2.3 \times 10^4$ – $9.6 \times 10^5$ cells/gram) respectively (Figure 6A) in reasonable agreement with previous estimates of ~$5 \times 10^4$/g in LN of HIV-infected patients in the USA with a mean CD4+ T cell count of 400 cells/μl[16]. However, this is more than ten-fold lower than observed in the SIVmac251-infected RM necropsied at 90 dpi.

To determine the size of the vDNA+ cell population before ART in relation to vRNA+ cells (as an estimate of cells with transcriptionally competent proviruses in these snapshots), we performed DNAscope and RNAscope in LN and rectum specimens. Before ART, the mean frequency of vDNA+ cell in LN was ~$6.2 \times 10^7$ vDNA+ cells/gram LT (range $8.3 \times 10^6$ –

$1.3 \times 10^6$) (Figure 6B), and thus the ratio of vRNA+ cells to vDNA+ cells was ~0.002, in good agreement with ratios of 1:100 to 1:400 in previous studies using *in situ* PCR and ISH[2].

ART had a significant impact on the LT reservoir in individuals who had been treated for > 2 years (range 2-6 years) and had undetectable plasma viral loads (<40 copies/ml in the first 12 months of the study and then <20 copies/ml). The mean frequency of vDNA+ cells declined by ~3 logs to ~$2.7 \times 10^5$ cells/gram (range $1.2 \times 10^5 – 4.5 \times 10^5$ cells/gram, $p = 0.0237$, ANOVA). In gut tissues, however, we did not document any significant decrease in the size of the vDNA+ cell reservoir (Figure 6C): prior to ART the frequency of vDNA+ cells were ~$3.2 \times 10^5$ cells/gram LT (range $2.8 \times 10^5 – 3.4 \times 10^5$) compared to a mean of ~$2.7 \times 10^5$ cells/gram (range $1.5 \times 10^5 – 4.3 \times 10^5$ cells/gram) after >62 months of ART (range 2-6 years, $p > 0.05$).

## Discussion

Using contemporary ISH methodologies to analyze tissue virus burdens as populations of infected cells, we have confirmed the paramount importance of the LT reservoir before treatment and during ART. These technologies also notably revealed during ART, that vRNA + and virus producing cells persist in tissues with plasma viremia of less than 50 copies/mL. Thus, our findings suggest that tissue assessments will be needed to fully determine the effectiveness of interventions designed to cure for HIV infection.

In the NHP models where we could comprehensively analyze key organ systems in a way that would not be possible in HIV-infected humans, ~99.6% of SIV RNA+ cells were found in LTs (LNs, gut, spleen and lung). Thus, there is now compelling additional evidence to support the conclusion that lymphoid organs comprise the principal tissue sites for virus production[7]. In the heart, liver, and kidney, the frequencies of vRNA+ cell were very low, but we did find vRNA+ cells in brain (cortex) at a frequency of ~$2.3 \times 10^4$ cells/gram and the frequency was comparable or higher in animals on ART, consistent with a potentially important role for the brain as a site of viral persistence that may not be as amenable to viral suppression on ART as peripheral tissues, at least with the antiretrovirals employed in the present study[27,28].

In both SIV-infected animals and in HIV-infected individuals, ART suppressed viral replication as judged by plasma vRNA measurements, but we readily detected vRNA+ and virus producing cells in tissues, albeit at reduced frequencies compared to untreated animals. This evidence for continued low level viral production despite ostensibly suppressive ART was correlated particularly in gut with the lower relative concentrations of ARVs in tissues compared to PBMCs documented in these studies. Notably, our results are consistent with the conclusions from studies of HIV infection that suboptimal tissue levels of ARVs in some treated infected individuals may not fully suppress virus production in tissues[5,20]. In the Ugandan cohort, other factors such as tissue fibrosis, persistent GI tract damage and associated inflammation and greater CD4+ T cell depletion in advanced stages of infection at the time ART was initiated[29-33] could also have contributed to ongoing infection by

further lowering drug levels and impairing containment of infection by the damaged immune system.

Finding vRNA+ cells in tissues during ART does not distinguish between low levels of ongoing virus production and reactivating latently infected cells. What we can say from the estimated quasi steady state whole body burden of 7 million vRNA+ cells in lymphoid tissues snapshots in people on suppressive ART for > 2 years is that either or both reservoirs are large immediate sources of virus to reignite infection after treatment interruption. This conclusion is supported by the rapid multifocal rebound in LT with genetically diverse viruses with treatment interruption[19] in HIV infected persons on ART for an average of 14.6 years; and with estimates here of the size of the pool of latently infected cells harbouring replication competent and inducible proviruses. We find a frequency of vDNA+ cells maintained in the LT reservoir at levels of ~$10^5$ vDNA+ cells/g despite ART in both SIV and HIV infections. If, as recent estimates suggest[21], only ~5% of vDNA+ cells have replication competent and inducible proviruses, the total body burden of latently infected cells with potentially inducible replication competent proviruses would be ~$4 \times 10^8$ cells. This estimate is in excellent agreement with measurements by Bruner *et al.* whose sequence analysis suggested a population of ~$1.2 \times 10^7$ resting memory cells in PBMC harbor replication competent provirus[34]. Given that less than 5% of resting memory cells are in peripheral blood, the frequency of vDNA+ cells in LTs with replication competent provirus would be on the order of ~$2.4 \times 10^8$ cells. Thus, two independent methods converge on similar estimates of a very large potentially inducible reservoir in patients on current ART regimens.

Both ongoing low level virus production due to lower concentrations of ARVs in LTs and reactivation of latently infected cells provide potential sources of virus that may rapidly reignite infection following treatment interruption. It will be important in future studies to develop and evaluate cure strategies that effectively target each source. For ongoing virus production, we need fully suppressive ART for LT and other tissue sites. For the latently infected inducible population, we need strategies with significantly greater impact than current latency reversal agents afford, coupled with effective means to eliminate the reactivated cells.

## Methods

### Clinical and Laboratory Analysis (Humans)

HIV-infected people in Kampala, Uganda who were eligible to start ART were recruited into a longitudinal protocol that was conducted at the Joint Clinical Research Center (JCRC). All subjects gave written informed consent and the Institutional Review Boards (IRB) of the University of Minnesota and JCRC and the Uganda National Council of Science and Technology (UNCST) approved the study. This was a longitudinal pathogenesis based study with no pre-determined comparators, as such we did not have a pre-determined sample size for recruitment.

### Study Procedures

At screening, peripheral blood was obtained to determine CD4 T cell count and plasma HIV RNA. Just prior to ART initiation, all participants had an excisional inguinal lymph node biopsy, after which they were started on an ART regimen consisting of two nucleoside reverse transcriptase inhibitors (NRTI) and one non-NRTI, as per the Uganda national HIV treatment guidelines. Subsequent CD4 T cell counts and HIV RNA levels were measured every 6 months to monitor treatment response. Lymph node and rectal biopsies were repeated at 12, 24, and 36 months of follow up.

### Clinical and Laboratory Analysis (NHP)

Tissues used in the described NHP studies were obtained from pre-existing tissue banks or were part of additional approved studies. As such, there were no formal sample-size estimates made prior to study design. No randomization was used to select animals for the study and the inclusion/exclusion criteria are described below. The investigators were not blinded to which group animals were from or to their infection history or treatment regimen and duration was.

### Animals and SIV infection

Rhesus macaques of Indian origin (*Macaca* mulatta; RMs) used for SIV infection in these studies were mature male and female animals ranging in age from approximately 3-12 years, and were negative for MHC alleles associated with SIV control (Mamu A*01, B*08, and B*17). Eight RMs were housed at Advanced Bioscience Laboratories (ABL) in accordance with the Association for the Assessment and Accreditation of Laboratory Animal Care (AAALAC) standards and all procedures were performed according to protocols approved by the ABL Institutional Animal Care and Use Committee (IACUC) (Protocol # AUP504, OLAW Assurance #A3467-01) Animals at ABL were intravenously (i.v.) inoculated with either $1.9 \times 10^4$ $TCID_{50}$ SIVmac251 (generated in the laboratory of Dr. Ron Desrosiers during 2006) or 100 $TCID_{50}$ SIVmac251 (generated in 2010 in the laboratory of Dr. Ron Desrosiers Three RMs (P568, P096, and P533) were infected with SIVmac251 (no ART) and sacrificed at 14, 43, and 90 days post infection. Five additional RMs (R365, R366, R367, R406 and R410) were infected with SIVmac251 and placed on ART at 8 wpi started on an ART regimen that consisted of the NRTIs tenofovir (PMPA; 20 mg/kg; Gilead Biosciences) and emtricitabine (FTC; 50 mg/kg; Gilead Biosciences) administered subcutaneously, and the integrase strand transfer inhibitor raltegravir (RAL; 150mg BID) plus the protease inhibitors darunavir (DRV; 400 mg; BID) and ritonavir (RTV; 100 mg; BID) given orally; and treated for 20-22 weeks prior to being sacrificed. These 8 RMs were utilized to perform a comprehensive tissue analysis of where SIV persisted in untreated and ART treated infection.

The experimental conditions and ART regimens employed for the 11 rhesus macaques housed at the National Cancer Institute were previously described for 5 RM (DCCN, DCHV, DCT3, DCEG, and DCJB) which received 26-32 weeks of ART beginning at 4 weeks post-infection and 6 RM (DCLJ, DCT2, DCEA, DC1G, DCCP and DCEW) which received a different regimen and also begun at 4 weeks post-infection, for 31-32 weeks[22,24,25] Lymph nodes were collected by surgical extraction before (4 wpi) and 26-32 weeks after the

initiation of ART (30-40 wpi) and immediately fixed in freshly prepared neutral buffered 4% paraformaldehyde (PFA) for 24 h at room temperature. After fixation for 24 h, fixative was replaced with 80% ethanol and tissues were paraffin embedded as previously described [25].

## Animals and RT-SHIV Infection

All animals were from the retrovirus-free colony of the California National Primate Research Center (CNPRC), which operates according to the Guide for the Care and Use of Laboratory Animals prepared by the Committee on Care and Use of Laboratory Animals of the Institute of Laboratory Animal Resources, National Research Council. The studies were approved by the University of California, Davis Institutional Animal Care and Use Committee (IACUC). The University of California, Davis is accredited by the Association for Assessment and Accreditation of Laboratory Animal Care, International (AAALAC). The University of California, Davis has an Animal Welfare Assurance on file with the Office of Laboratory Animal Welfare (OLAW).

Stocks of RT-SHIV were prepared as described previously [26]. The RT-SHIV used has the T-to-C substitution at position 8 of the SIV tRNA primer binding site, which is necessary for efficient replication of RT-SHIV *in vivo*. Juvenile rhesus macaques (*Macaca mulatta*) 7 to 10 months of age (~2.0 to 3.1 kg) were used in the RT-SHIV study as described by North et al. [26] Efavirenz (200 mg per day) was given in food. The NRTIs PMPA and FTC were administered subcutaneously, with a regimen of 16 mg per kg of body weight once daily for FTC and 30 mg per kg of body weight once daily for PMPA. The dose of PMPA was reduced to 15 mg/kg per day after 20 weeks of treatment to reduce potential long-term renal toxicity associated with prolonged administration at the higher dose.

## CD4 T cell count analysis

Macaques: EDTA-treated whole blood was stained using CD3, CD4, and CD8 monoclonal antibodies and analyzed using a BD FACSCalibur Flow Cytometer (BD Biosciences, San Jose, CA). Cell counts were determined using the BD Trucount tubes according to the manufacturer's instructions (BD Biosciences, San Jose, CA).

Humans: Blood CD4 cells counts were measured at the same time-points by flow cytometry using FACSCount™ (Becton Dickinson Inc, Franklin Lakes, NJ, USA).

## Quantitation of plasma viral RNA load

Macaques: Plasma isolated from EDTA-blood of SIVmac251 infected RM was clarified by centrifugation at 2300 × g for 3 minutes. The clarified plasma (0.1 mL) was then lysed directly in lysis buffer (bioMerieux, Durham, NC, USA). Alternatively, a higher volume of plasma (0.5 to 1 ml) was centrifuged to pellet virus by ultracentrifugation at 49 100 × g for 60 min and the pellet lysed in lysis buffer. Viral RNA load in the lysed samples was quantitated using Real-time NASBA assay as described elsewhere [35]. Plasma SIVmac239/251 viral loads were determined as described, with an assay threshold of 30 copies/mL[24,25] Plasma isolated from the blood of RT-SHIV infected challenged macaques was analyzed using previously described methods [26] where the lower limit of detection was 5 copies/ml.

Humans: Plasma HIV viral load was measured using the COBAS Ampliprep/COBAS TaqMan 96 (Roche, Branchburg, NJ, USA) with a linearity range of 20-10,000,000 copies/ml or Abbott m2000 system platform with a linearity range of 40-10,000,000 copies/ml. The Abbott platform was used in the first 12 months of the study and the Roche for all subsequent measures. Both platforms were registered on an external quality assurance program provided by the American Pathologists and Virology Quality Assurance from RUSH University Medical Center.

## Procedures for Initial Tissue Management

At the time of biopsy, LN was dissected into 2 pieces. Half was transferred to 4% paraformaldehyde (PFA) for 4-6 hours, then washed in 80% ethanol and embedded in paraffin and subsequently sectioned in 4 micron sections for ISH analysis.

## *In situ* hybridization

These methods have been previously described. Briefly, for the radio-labeled and RNA/DNAscope techniques a total of three to five 4μ sections separated by 20μ are analyzed by one of 3 *in situ* hybridization methods. For ISH/TSA/ELF 10μ sections are used.

**Radio-labeled ($^{35}$S) *In situ* methods—**Sections were hybridized at 45C overnight with a $^{35}$S labeled riboprobe and 0.5mM aurintricarboxylic acid in the hybridization mix using methods we have previously described[16]. After extensive washes and ribonuclease treatment, tissue sections were dehydrated, coated in emulsion and exposed at 4C for 7-14 days.

**ISH/TSA/ELF—**These methods have been previously described[23,36]. Briefly, sections are hybridized to digoxingenin-labelled HIV specific antisense riboprobes with 0.5mM aurintricarboxylic acid to reduce background. After hybridization, tissues are incubated with anti-digoxigenin Ab conjugated with HRP, extensively washed, and then incubated with biotinyl tyramine to amplify signals. The amplification step was repeated 3 times to detect virus particles. Tissues were then treated with streptavidin-alkaline phosphatase and RNA signals were visualized with fluorescent ELF97 alkaline phosphatase substrate.

**RNAscope/DNAscope—**The anti-sense (for the detection of vRNA) and sense (for the detection of vDNA) SIV and HIV probes used covers ~4.5kb of the genome and are designed to bind to sequences in *gag*, *pol*, *vif, vpx* (for SIV), *vpr, tat, rev, vpu* (for HIV) *env* and *nef* as previously described [22].

## Quantitative Image Analysis

Photographic images are captured and the frequency of vRNA+ or vDNA+ cell measured and expressed as the total per unit area. These methods have been extensively reviewed[14,18,37].

## Quantitation of Antiretroviral Drug Concentrations

Intracellular concentrations of TFV-DP, FTC-TP, DRV and RTV were quantified from lysed cellular matrix from PBMCs, and MNCs obtained from biopsy samples of the LN, ileum

(GALT), and rectum (RALT) using methods previously described[5,38]. Final sample extracts were quantified with a liquid chromatography–triple quadrupole mass spectrometer system consisting of a Shimadzu Nexera ultra high-performance liquid chromatograph attached to an AB Sciex 5500 QTrap mass spectrometer. Quality control sample interbatch coefficients of variance for the TFV-DP and FTC-TP and the DRV and RTV methods were 3.84–7.67% and 1.1–7.4%, respectively. Absolute mean relative errors to the theoretical target quality control samples were <5.6% for TFV-DP and FTC-TP and <8.1% for DRV and RTV. Batch acceptance criterion was derived according to the Food and Drug Administration Guidance for Industry on Bioanalytical Method Validation[39]. Results from intracellular analysis were expressed in femtomoles per million cells. Relative penetration of the ARVs into the LN, GALT and RALT was assessed as a ratio of concentrations to those in PBMCs.

### Statistical Analysis

Data presented from individual animals to describe the frequency of vRNA or vDNA+ cell are expressed as the total number of cells/gram tissue for that organ in that animal (e.g., Figures 2 and 3). Analysis of differences between tissue sites, or before and during ART, were made by comparing the means of the two groups using ANOVA (e.g., Figure 6).

## Supplementary Material

Refer to Web version on PubMed Central for supplementary material.

## Acknowledgments

The authors would like to thank Scott Povolny and Craig Olson for their help with manuscript preparation and editing and the Antiviral Pharmacology Laboratory at the University of Nebraska for quantitation of antiretroviral drug concentrations. This work was supported by the following grants: UL1TR000114, AI096109, OD011107, AI124965, and AI074340, and in part with federal funds from the National Cancer Institute, National Institutes of Health, under Contract No. HHSN261200800001E. The content of this publication does not necessarily reflect the views or policies of the Department of Health and Human Services, nor does mention of trade names, commercial products, or organizations imply endorsement by the U.S. Government.

## References

1. Yukl SA, et al. Challenges in detecting HIV persistence during potentially curative interventions: a study of the Berlin patient. PLoS Pathog. 2013; 9:e1003347. [PubMed: 23671416]
2. Embretson J, et al. Analysis of human immunodeficiency virus-infected tissues by amplification and in situ hybridization reveals latent and permissive infections at single-cell resolution. Proceedings of the National Academy of Sciences of the United States of America. 1993; 90:357–361. [PubMed: 8419941]
3. Embretson J, et al. Massive covert infection of helper T lymphocytes and macrophages by HIV during the incubation period of AIDS [see comments]. Nature. 1993; 362:359–362. [PubMed: 8096068]
4. Faust RA, et al. Outpatient biopsies of the palatine tonsil: access to lymphoid tissue for assessment of human immunodeficiency virus RNA titers. Otolaryngology Head & Neck Surgery. 1996; 114:593–598. [PubMed: 8643270]
5. Fletcher CV, et al. Persistent HIV-1 replication is associated with lower antiretroviral drug concentrations in lymphatic tissues. Proc Natl Acad Sci U S A. 2014; 111:2307–2312. [PubMed: 24469825]
6. Haase AT. Population biology of HIV-1 infection: viral and CD4+ T cell demographics and dynamics in lymphatic tissues. Annual review of immunology. 1999; 17:625–656.

7. Reinhart TA, et al. Simian immunodeficiency virus burden in tissues and cellular compartments during clinical latency and AIDS. J Infect Dis. 1997; 176:1198–1208. [PubMed: 9359719]
8. Reinhart TA, et al. A new approach to investigating the relationship between productive infection and cytopathicity in vivo. Nature Medicine. 1997; 3:218–221.
9. Chomont N, et al. HIV reservoir size and persistence are driven by T cell survival and homeostatic proliferation. Nat Med. 2009; 15:893–900. [PubMed: 19543283]
10. Chun TW, et al. Quantification of latent tissue reservoirs and total body viral load in HIV-1 infection. Nature. 1997; 387:183–188. [PubMed: 9144289]
11. Chun TW, et al. Rebound of plasma viremia following cessation of antiretroviral therapy despite profoundly low levels of HIV reservoir: implications for eradication. AIDS. 2010; 24:2803–2808. [PubMed: 20962613]
12. Chun TW, et al. HIV-infected individuals receiving effective antiviral therapy for extended periods of time continually replenish their viral reservoir. J Clin Invest. 2005; 115:3250–3255. [PubMed: 16276421]
13. Pantaleo G, et al. Lymphoid organs function as major reservoirs for human immunodeficiency virus. Proceedings of the National Academy of Sciences of the United States of America. 1991; 88:9838–9842. [PubMed: 1682922]
14. Schacker T, et al. Rapid accumulation of human immunodeficiency virus (HIV) in lymphatic tissue reservoirs during acute and early HIV infection: implications for timing of antiretroviral therapy. J Infect Dis. 2000; 181:354–357. [PubMed: 10608788]
15. Schnittman SM, et al. The reservoir for HIV-1 in human peripheral blood is a T cell that maintains expression of CD4. Science. 1989; 245:305–308. [PubMed: 2665081]
16. Haase AT, et al. Quantitative image analysis of HIV-1 infection in lymphoid tissue. Science. 1996; 274:985–989. [PubMed: 8875941]
17. Li Q, et al. Peak SIV replication in resting memory CD4+ T cells depletes gut lamina propria CD4+ T cells. Nature. 2005; 434:1148–1152. [PubMed: 15793562]
18. Schacker T, et al. Productive infection of T cells in lymphoid tissues during primary and early human immunodeficiency virus infection. J Infect Dis. 2001; 183:555–562. [PubMed: 11170980]
19. Rothenberger MK, et al. Large number of rebounding/founder HIV variants emerge from multifocal infection in lymphatic tissues after treatment interruption. Proc Natl Acad Sci U S A. 2015; 112:E1126–1134. [PubMed: 25713386]
20. Lorenzo-Redondo R, et al. Persistent HIV-1 replication maintains the tissue reservoir during therapy. Nature. 2016; 530:51–56. [PubMed: 26814962]
21. Ho YC, et al. Replication-competent noninduced proviruses in the latent reservoir increase barrier to HIV-1 cure. Cell. 2013; 155:540–551. [PubMed: 24243014]
22. Deleage C, et al. Defining HIV and SIV Reservoirs in Lymphoid Tissues. Pathogens and Immunity. 2016; 1:68–96. [PubMed: 27430032]
23. Reilly C, Wietgrefe S, Sedgewick G, Haase A. Determination of simian immunodeficiency virus production by infected activated and resting cells. Aids. 2007; 21:163–168. [PubMed: 17197806]
24. Del Prete GQ, et al. Elevated Plasma Viral Loads in Romidepsin-Treated Simian Immunodeficiency Virus-Infected Rhesus Macaques on Suppressive Combination Antiretroviral Therapy. Antimicrobial Agents And Chemotherapy. 2015; 60:1560–1572. [PubMed: 26711758]
25. Del Prete GQ, et al. Effect of suberoylanilide hydroxamic acid (SAHA) administration on the residual virus pool in a model of combination antiretroviral therapy-mediated suppression in SIVmac239-infected indian rhesus macaques. Antimicrobial Agents And Chemotherapy. 2014; 58:6790–6806. [PubMed: 25182644]
26. North TW, et al. Viral sanctuaries during highly active antiretroviral therapy in a nonhuman primate model for AIDS. J Virol. 2010; 84:2913–2922. [PubMed: 20032180]
27. Clements JE, et al. The central nervous system as a reservoir for simian immunodeficiency virus (SIV): steady-state levels of SIV DNA in brain from acute through asymptomatic infection. J Infect Dis. 2002; 186:905–913. [PubMed: 12232830]
28. Clements JE, et al. The central nervous system is a viral reservoir in simian immunodeficiency virus–infected macaques on combined antiretroviral therapy: a model for human

immunodeficiency virus patients on highly active antiretroviral therapy. J Neurovirol. 2005; 11:180–189. [PubMed: 16036796]

29. Estes J, et al. Collagen deposition limits immune reconstitution in the gut. J Infect Dis. 2008; 198:456–464. [PubMed: 18598193]
30. Estes JD, Haase AT, Schacker TW. The role of collagen deposition in depleting CD4+ T cells and limiting reconstitution in HIV-1 and SIV infections through damage to the secondary lymphoid organ niche. Seminars-in-immunology. 2008
31. Schacker TW, et al. Lymphatic tissue fibrosis is associated with reduced numbers of naive CD4+ T cells in human immunodeficiency virus type 1 infection. Clin Vaccine Immunol. 2006; 13:556–560. [PubMed: 16682476]
32. Schacker TW, et al. Collagen deposition in HIV-1 infected lymphatic tissues and T cell homeostasis. J Clin Invest. 2002; 110:1133–1139. [PubMed: 12393849]
33. Schacker TW, et al. Amount of lymphatic tissue fibrosis in HIV infection predicts magnitude of HAART-associated change in peripheral CD4 cell count. AIDS. 2005; 19:2169–2171. [PubMed: 16284469]
34. Bruner KM, et al. Defective proviruses rapidly accumulate during acute HIV-1 infection. Nat Med. 2016; 22:1043–1049. [PubMed: 27500724]
35. Lee EM, et al. Molecular methods for evaluation of virological status of nonhuman primates challenged with simian immunodeficiency or simian-human immunodeficiency viruses. Journal Of Virological Methods. 2010; 163:287–294. [PubMed: 19878696]
36. Zhang ZQ, et al. Roles of substrate availability and infection of resting and activated CD4+ T cells in transmission and acute simian immunodeficiency virus infection. Proc Natl Acad Sci U S A. 2004; 101:5640–5645. [PubMed: 15064398]
37. Cavert W, et al. Kinetics of response in lymphoid tissues to antiretroviral therapy of HIV-1 infection. Science. 1997; 276:960–964. [PubMed: 9139661]
38. Podany AT, Winchester LC, Robbins BL, Fletcher CV. Quantification of cell-associated atazanavir, darunavir, lopinavir, ritonavir, and efavirenz concentrations in human mononuclear cell extracts. Antimicrobial Agents And Chemotherapy. 2014; 58:2866–2870. [PubMed: 24614370]
39. Guidance for Industry: Bioanalytical Method Validation, U.S.D.o.H.a.H Services. Rockville, Md: 2001. (ed. 2001 E.)
40. Fremming BD, Benson RE, Young RJ. Weights of organs in sixty-six male Macaca mulatta monkeys. J Appl Physiol. 1955; 8:155–158. [PubMed: 13263256]

**One sentence summary**

During suppressive ART, sources of virus from which infection can rebound when treatment is interrupted persist in lymphoid tissue reservoirs, where there are potentially more than $10^8$ viral DNA+ cells that could be reactivated, and virus-producing cells in low drug level sanctuaries.

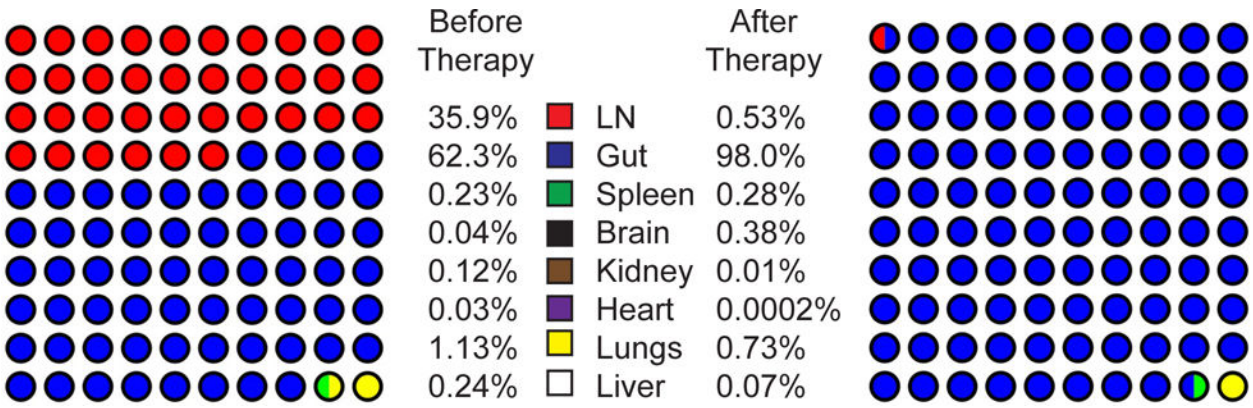


**Figure 1.**
Graphical representation of proportion of vRNA+ cells in each organ system before and during suppressive ART.

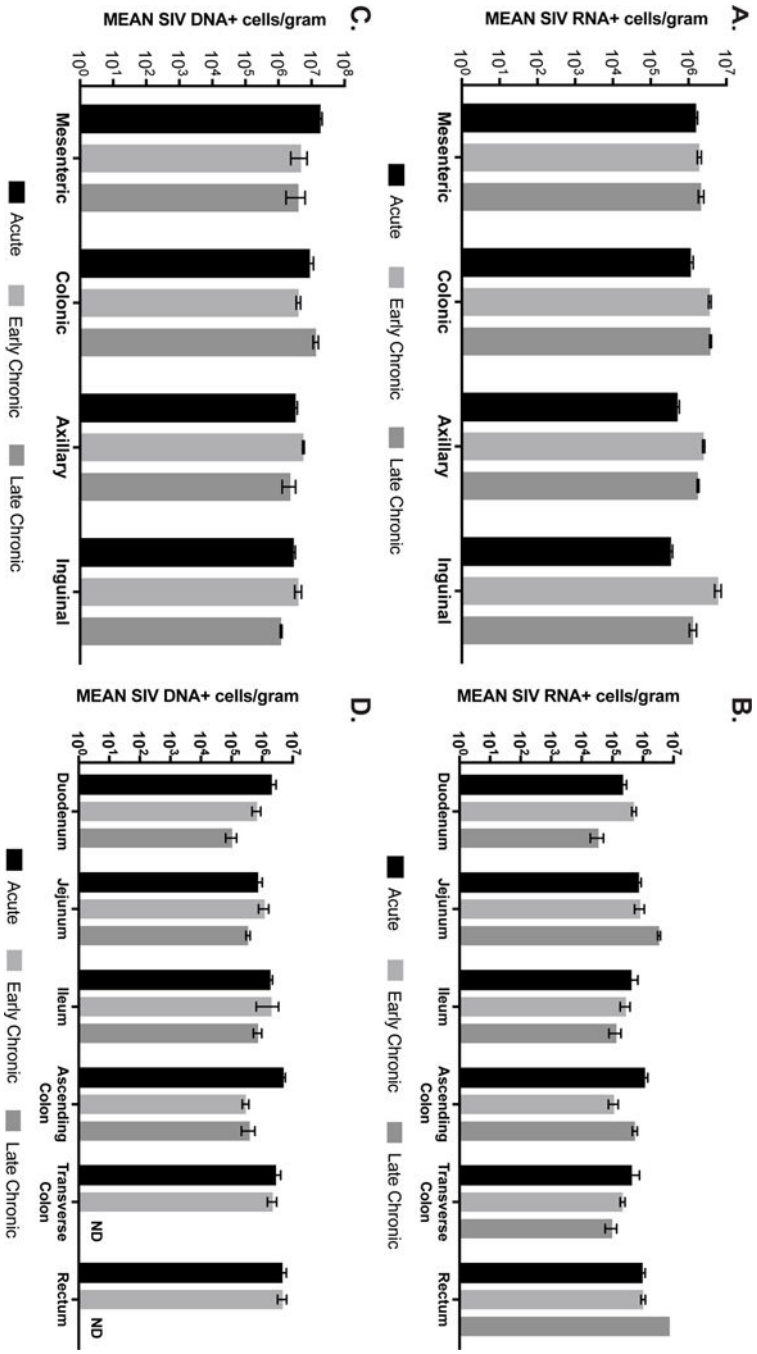


**Figure 2.**

Quantitative image analysis of SIV vRNA+ cells in untreated SIV infection. A, B. Estimated frequency of vRNA+ cells/gram tissue in LN and gut associated LT in an animal sampled during acute, early chronic and late chronic stage of infection. C, D. Estimated frequency of SIV DNA+ cells in 4 different LN and 7 sites in GALT at each stage of SIV infection from the same animals. Each value is from a single LN from a single animal where an average of 5 sections is made. The error bars represent the SEM of the 5 measures.

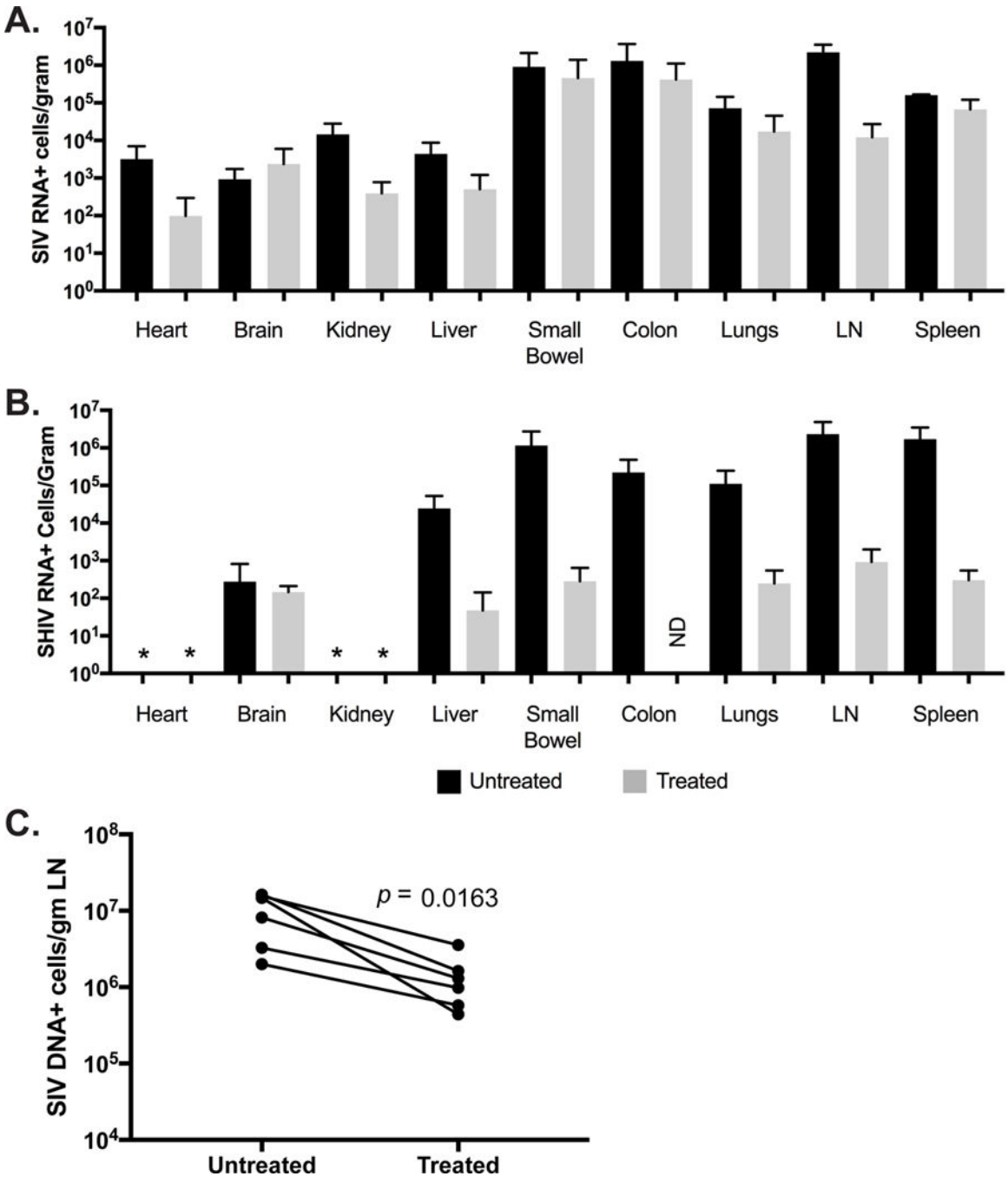


**Figure 3.**

Quantitative image analysis of vRNA+ and vDNA+ cells in groups of untreated and treated SIV and SHIV infection. A. Frequency (mean frequency and s.d.) of SIVmac251 RNA+ cells in untreated RM (animals euthanized at 14, 43, and 90 dpi) and RM after receiving 20-22 weeks of ART started at 56 dpi. B. Frequency of vRNA+ cells in RT-SHIV infected animals after 26 weeks of ART C. Frequency of SIV DNA+ cells in paired lymph nodes of 5 SIVmac239 infected macaques before and after 26 weeks of ART (comparison by paired t test). * means the tissue was not available and ND means none detected.

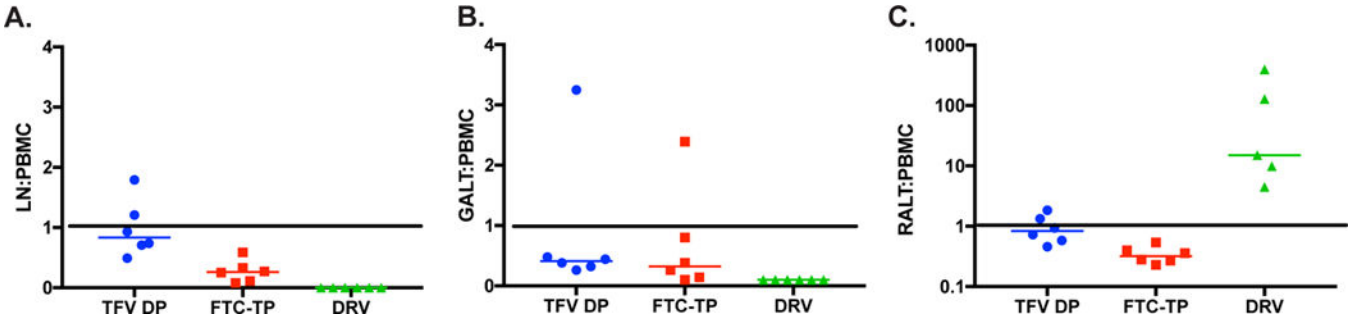


**Figure 4.**

Intracellular concentrations of TFV-DP, FTC-TP, and DRV in LN, gut, and rectum compared with simultaneous measures in PBMC in six macaques. A. LN:PBMC. B. Gut:PBMC. Rectum:PBMC. Median concentration is indicated.

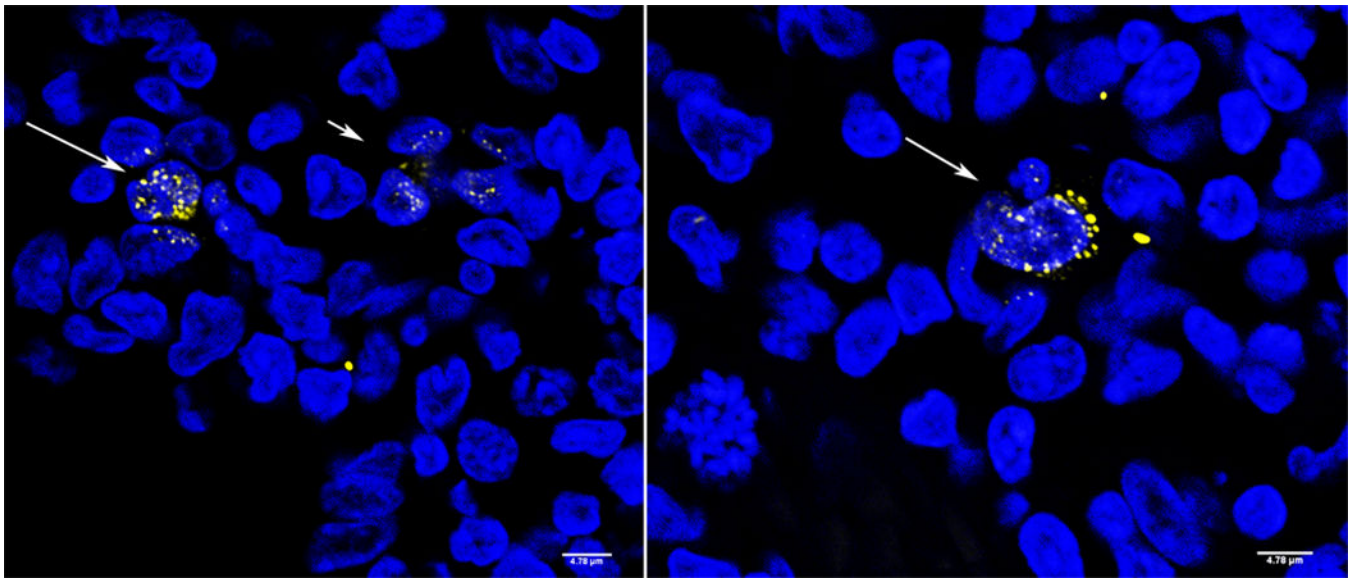

**Figure 5.**

Virus-producing cells in two SIV-infected rhesus macaques during ART detected by ISH/TSA. In the left panel, the long arrow points to two virus-producing cells; the short arrow points to a cluster of four productively infected cells. In the right panel, the arrow points to two productively infected cells. Virus particles appear yellow; cell nuclei are blue. Multiphoton Images obtained at z steps of 0.1 microns and subsequently filtered to reduce the intracellular viral RNA staining so that virus particles were visible. The sizes of virions depend on the plane of focus; larger virions are in focus.

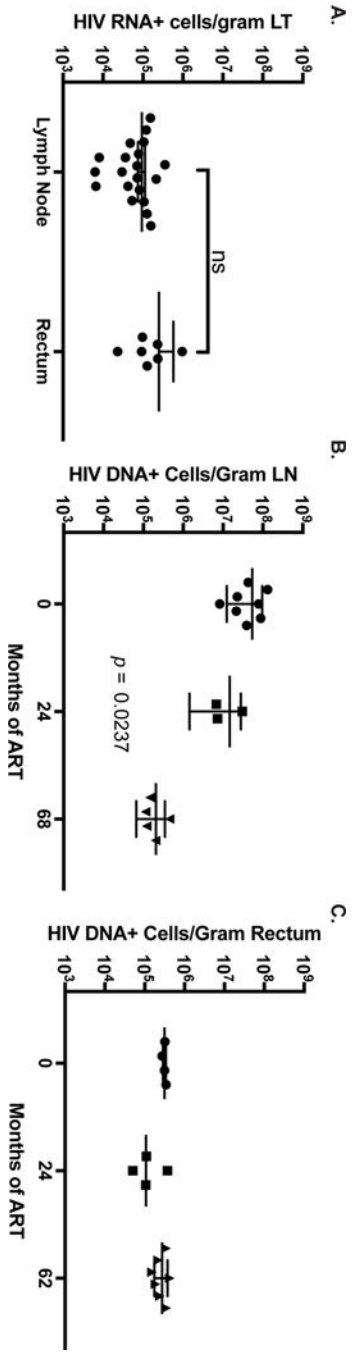


**Figure 6.**

Frequency of vRNA and vDNA+ /gram in HIV+ Ugandans before and during ART in LN and rectal biopsies. A. Frequency of HIV RNA+ cell/gram LN compared to the frequency in rectum (unpaired t test). B, C. Frequency of DNA+ cells in LN and rectum versus months of ART (One-way ANOVA).